Enumeration of Isobaric Inherent Structures for the Fragile Glass Former *o*-Terphenyl

Frank H. Stillinger

Bell Laboratories, Lucent Technologies Inc., Murray Hill, New Jersey 07974, and Princeton Materials Institute, Princeton University, Princeton, New Jersey 08544

Received: September 29, 1997; In Final Form: January 30, 1998

The widely investigated organic substance *o*-terphenyl (OTP) displays thermal and kinetic behavior prototypical for "fragile" glass formers. The special relationship between its heat capacity in supercooled liquid, amorphous glass, and crystalline solid states provides simple access to the enumerating distribution function for its amorphous inherent structures (potential energy minima) by depth. The thermodynamic calculations required at 1 atm yield a broad and somewhat asymmetric distribution. This distribution implies that supercooling OTP from its melting point (329.35 K) to its glass transition (240 K) succeeds only in reducing inherent structure enthalpy by 66% of the amount that would be required to attain the most stable amorphous inherent structure.

I. Introduction

Experimental data on glass-forming substances are vast and diverse. To help organize all of this empirical information, Angell has suggested that these substances be placed along a scale between "strong" and "fragile" extremes.[1−3] The former displays Arrhenius temperature dependence for its liquid-phase shear viscosity and no sharp changes in thermodynamic properties through the glass transition region. By contrast, the latter possesses strong deviations from Arrhenius behavior of its shear viscosity and exhibits sudden and vivid changes in thermodynamic behavior across a sharply defined glass transition. In particular, the heat capacity of a supercooled liquid near the fragile extreme undergoes a nearly discontinuous drop as the temperature declines through T_g, the glass transition temperature.

o-Terphenyl (OTP) has become one of the most intensively and frequently examined of the fragile glass formers and is often cited as the archetypal illustration of the fragile extreme. Its behavior doubtless stems, at least in part, from nonrigidity of the individual molecules and from the relatively nondirectional forces acting between neighboring molecules. A sampling of its experimental literature reveals determinations of crystal structure,[4,5] heat capacity,[6] viscosity,[7,8] thermal conductivity,[9] light scattering,[10] and translational and rotational diffusion rates.[11]

The existence of glass transitions for deeply supercooled liquids is generally conceded to be a phenomenon of kinetic arrest.[3,12,13] As temperature declines, the collection of configurational coordinates describing the molecules in such a liquid move into, and become increasingly trapped within, regions of the multidimensional configuration space characterized by deep potential energy minima and high intervening barriers. Theory has the obligation to infer geometric details of this "rugged potential energy landscape" and to show how those details vary from substance to substance.

The present study focuses primarily on one aspect of rugged potential energy hypersurfaces. Specifically, this entails enumeration (for OTP) of local minima (mechanically stable molecular packings), to be called "inherent structures" in the following. It will be shown that the available heat capacity data for OTP[6] allows extraction of the asymptotic (large-system limit) distribution of inherent structures by depth.

Section II briefly reprises for completeness the essential elements of inherent structure theory, specifically for isobaric (constant pressure) conditions that apply to most experiments. Section III provides a critical appraisal of the best available heat capacity data for OTP[6] and argues that its form strongly suggests a simple route to the asymptotic enumerating distribution. Section IV presents details of the elementary calculations required to produce that distribution and shows their results. Finally, section V discusses the extension of the present analysis to other glass formers, examines its relation to the so-called Kauzmann paradox[14,15] and comments on other aspects of the rugged potential energy hypersurface probed by a wide variety of kinetic measurements.

II. Inherent Structure Formalism

Consider for the moment an arbitrary condensed matter system comprising N particles (atoms, ions, or molecules). Vector $\mathbf{r}_i$ will represent the configurational coordinates for the ith particle, and depending on the case of interest, it will specify position, orientation, and internal configurational state. The volume V available to this system is determined by the container's wall forces.

Let $\Phi(\mathbf{r}_1, ..., \mathbf{r}_N, V)$ stand for the potential energy function. It will include intramolecular conformational energy, interparticle interactions (which may not be pairwise additive), and interactions with the confining walls. Isochoric (constant V) inherent structures for the system are the mechanically stable arrangements of the N particles in the fixed container, corresponding to local minimization of Φ with respect to the configurational coordinates $\mathbf{r}_1, ..., \mathbf{r}_N$. Both generic arguments[16−18] as well as model-specific exact results[19,20] indicate that the number of distinct isochoric inherent structures rises exponentially with system size N, at constant density.

The majority of experiments that investigate glass-forming materials occur under isobaric (constant pressure, p), rather than isochoric, conditions. In this circumstance the volume V itself becomes a configurational variable. It is then natural to append pV to Φ, to form the "potential enthalphy" function:

S1089-5647(97)03144-1 CCC: $15.00
Published on Web 03/19/1998

$$\Psi(\mathbf{r}_1, ..., \mathbf{r}_N, V) = \Phi(\mathbf{r}_1, ..., \mathbf{r}_N, V) + pV \qquad (2.1)$$

Isobaric inherent structures at pressure p are local minima of Ψ over $\mathbf{r}_1$, ..., $\mathbf{r}_N$ *and* V. The number of such minima that are distinct is again expected to rise exponentially with respect to system size N.

Equilibrium statistical mechanics under isobaric conditions begins with the dimensionless partition function $\Delta(N,T,p)$ for the isothermal−isobaric ensemble.

$$\Delta = \exp(-\beta G)$$

$$= [K/\prod_{\alpha} N_\alpha!] \int d\mathbf{r}_1 ... \int d\mathbf{r}_N \int_0^\infty dV \, (\exp -\beta\Psi) \qquad (2.2)$$

Here $\beta = (k_B T)^{-1}$, G is the Gibbs free energy, and α indexes the separate particle species that are present. K is a normalizing constant whose V-independent value has no bearing on the following, but it should be noted in passing that it contains the inverse of a thermal deBroglie wavelength for the V-varying "piston" degree of freedom.

Arbitrary points in the $\mathbf{R} \equiv (\mathbf{r}_1, ..., \mathbf{r}_N, V)$ configuration space can be mapped onto the isobaric inherent structures by means of a weighted gradient descent equation:

$$\mathbf{w} \cdot (\partial \mathbf{R}/\partial s) = -\nabla \Psi(\mathbf{R}) \qquad (2.3)$$

where $s \geq 0$ is a progress variable for the descent, and $\mathbf{w}$ is a matrix of nonnegative weights. In the simple case that only one structureless particle species is present (i.e., N identical spherical particles), $\mathbf{w}$ can be replaced by the unit matrix. The mapping generated by eq 2.3 tiles the multidimensional $\mathbf{R}$ space with basins, one for each of the local Ψ minima (isobaric inherent structures). Specifically, the basin B_a surrounding minimum a is the collection of all points in $\mathbf{R}$ that map to a. Although variations in the elements of weight matrix $\mathbf{w}$ can influence the shapes of basins, their number is invariant to those variations.

The basin tiling of the space spanned by the partition function integrals, eq 2.2, leads to a simple formal transformation of Δ to an integral over a single variable, the depth of the basin minima on a per particle basis, ψ. In the asymptotic large-system limit, one finds the following result for the Gibbs free energy per particle in the case of a single species:

$$\beta G/N \sim (\ln K)/N + \beta\psi_m + \beta f(\beta, \psi_m) - \sigma(\psi_m) \qquad (2.4)$$

In this expression $f(\beta,\psi)$ is the mean intrabasin vibrational free energy per particle, for those basins with depth ψ; the density of inherent structures by depth is expressed by

$$\exp[N\sigma(\psi)] \qquad (2.5)$$

and ψ_m is the value of the intensive "order" parameter ψ that minimizes expression 2.4 under the prevailing temperature and pressure conditions.

In applying this representation to glass-forming substances that easily supercool and avoid transition to the crystal phase, a minor modification of eqs 2.4 and 2.5 is required. These systems (at least above the glass transition temperature) exhibit a restricted form of equilibrium, avoiding those basins whose inherent structures include some perceptible extent of crystalline order. After projecting these latter basins out of consideration, the corresponding version of Gibbs free energy eq 2.4 may be written with asterisks on the key quantities to indicate relevance to the liquid phase, both above and below the equilibrium melting temperature:

$$\beta G^*/N \sim (\ln K)/N + \beta\psi_m^* + \beta f^*(\beta, \psi_m^*) + \sigma^*(\psi_m^*) \qquad (2.6)$$

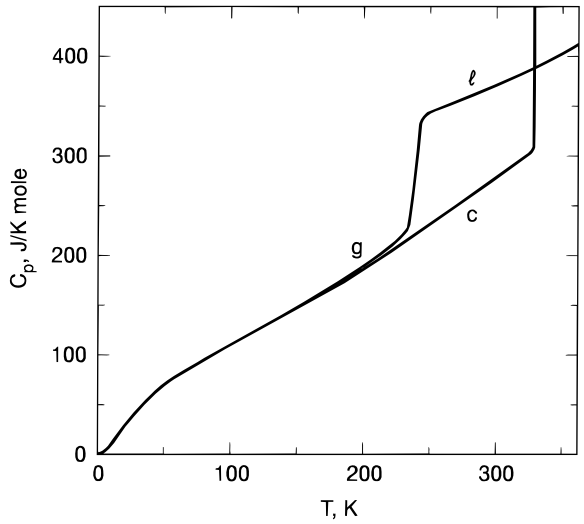

Figure 1. Constant-pressure heat capacity for OTP at 1 atm, redrawn from Chang and Bestul, ref 6, Figure 1.

Application to OTP requires identifying the relevant molecular degrees of freedom that should be included in each $\mathbf{r}_i$. It seems unnecessary to consider all intramolecular degrees of freedom, particularly the high-frequency vibrational motions. However, two angles that measure twist of the pendant benzene rings out of the plane of the central benzene ring are certainly relevant. Also, it can be argued that a symmetrical attachment-bond bend angle for displacement of those pendant rings relative to the central ring should be included. These must be joined by three Euler angles (or their equivalent) for overall molecular orientation in space and by three coordinates specifying translational position. Consequently, each $\mathbf{r}_i$ must contain a minimum of nine components.

III. Experimental Data

Figure 1, adapted and redrawn from Chang and Bestul,[6] shows the measured isobaric heat capacity $C_p(T)$ for OTP at 1 atm. Notable features are the following: (A) the crystal curve rises smoothly from 0 K to the melting point at $T_m = 329.35$ K, indicating no solid-state phase transitions; (B) the heat of fusion ΔH_m at T_m is 17 191 J mol^{-1}; (C) the liquid-phase heat capacity extrapolates smoothly through T_m into the supercooled regime, where it lies well above that for the crystal; (D) the supercooled liquid branch terminates abruptly at glass transition temperature $T_g \simeq 240$ K; (E) C_p for the glass over $0 < T < T_g$ lies only very slightly above that of the crystal.

These observations lead to conclusions that simplify the interpretation of the data. In particular, (E) indicates that the vibrational free energies of the crystal and the amorphous glass are very nearly equal; as a working assumption, we shall suppose that the difference is negligible. Note that quantum effects are substantial for vibrational degrees of freedom (particularly those of high frequency), but are equally present in crystal, glass, and liquid, so we can assume that their net effect on the quantities to be evaluated is negligible. Consequently, the heat capacity increment

$$\Delta C_p(T) = C_p^{(liq)}(T) - C_p^{(crys)}(T) \qquad (3.1)$$

over the range $T_g < T \leq T_m$ must be a direct measure of the temperature rate of change of $\psi_m^*(T)$ over the same range, since the crystal always inhabits the same basin, namely that for the absolute Ψ minimum (neglecting thermally induced point defects).

The experimental data in ref 6 giving $\Delta C_p(T)$ can be fitted accurately with the following simple formula:

$$\Delta C_p(T) \simeq A_2 T^{-2} + A_3 T^{-3} + A_4 T^{-4} \tag{3.2}$$

with deviations that appear to be comparable to the random measurement errors ± 0.01 J K^{-1} mol^{-1}). The optimized coefficients have values

$$A_2 = 2.023\,151\,951 \times 10^7 \text{ J K mol}^{-1}$$

$$A_3 = -4.617\,224\,704 \times 10^9 \text{ J K}^2 \text{ mol}^{-1}$$

$$A_4 = 3.234\,583\,582 \times 10^{11} \text{ J K}^3 \text{ mol}^{-1} \tag{3.3}$$

This fitting formula 3.2 can be used to infer ΔC_p values in experimentally inaccessible temperature ranges both above T_m and below T_g.

IV. Density of Inherent Structures

The favorable circumstances presented by the OTP heat capacity invite an attempt to extract its isobaric enumeration function σ^*. For this purpose, it is necessary to convert ΔC_p to specification of $\psi_m(T)$ and to the configurational (i.e., inherent structure) entropy as a function of temperature. Standard thermodynamics supplies these quantities subject to the conclusions presented in section II.

By assumption, the change in ψ due to melting is entirely equivalent to the heat of fusion. Consequently ψ_m^* at any other temperature, relative to its value for the crystal inherent structure, $\psi^{(cr)}$, can be expressed in terms of ΔH_m and an integral of C_p over the temperature interval from T_m:

$$\psi_m^*(T) - \psi^{(cr)} = \Delta H_m/N - \int_T^{T_m} \Delta C_p(T')\, dT'$$

$$\simeq 17\,191 - A_2(T^{-1} - {T_m}^{-1}) - \frac{1}{2}A_3(T^{-2} - {T_m}^{-2}) - \frac{1}{3}A_4(T^{-3} - {T_m}^{-3}) \tag{4.1}$$

where the latter form, expressed in terms of J mol^{-1}, results from inserting the experimental ΔH and the fitting formula 3.2.

A similar procedure yields the inherent structure entropy as a function of temperature, which is equivalent to specifying σ^*. First, note that at T_m this is given by the melting entropy. At other temperatures the difference appears as a familiar thermodynamic integral:

$$\Delta S(T)/Nk_B \equiv \sigma^*[\psi_m^*(T)]$$

$$= \Delta H_m/Nk_B T_m - \int_T^{T_m} [\Delta C_p(T')/T']\, dT'$$

$$= 52.20 - \frac{1}{2}A_2(T^{-2} - {T_m}^{-2}) - \frac{1}{3}A_3(T^{-3} - {T_m}^{-3}) - \frac{1}{4}A_4(T^{-4} - {T_m}^{-4}) \tag{4.2}$$

Units for the latter form are J K^{-1} mol^{-1}.

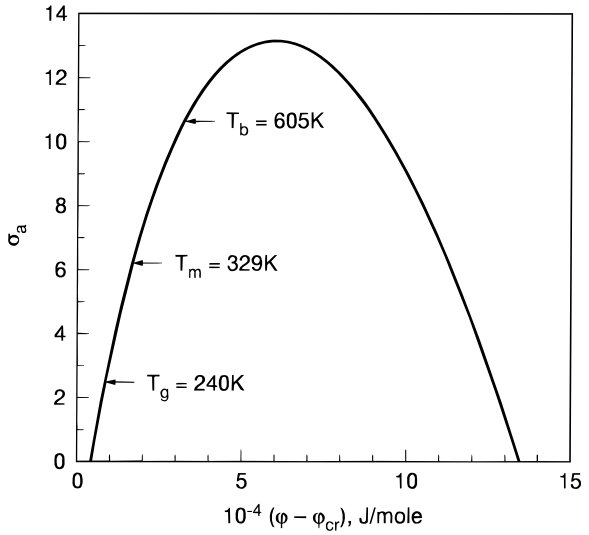

Figure 2. Isobaric enumeration function for OTP noncrystalline inherent structures. The pressure is 1 atm.

In principle, absolute temperature T could be eliminated between eqs 4.1 and 4.2. In practice, this can be accomplished numerically by simply evaluating both formulas over a wide range of temperatures and pairing the ψ_m^* and σ^* results. Figure 2 shows the outcome, where σ^* is plotted against $\psi - \psi^{(cr)}$. Several general points need to be stressed in connection with the curve shown.

(1) According to its definition, σ^* cannot be negative; consequently only that portion of the results from eqs 4.1 and 4.2 conforming to this constraint is shown in Figure 2.

(2) The left portion of the σ^* curve (displaying positive slope) corresponds to positive T, and its maximum corresponds to $T \rightarrow +\infty$. The right portion (negative slope) was traced out by using $T < 0$. This latter point entails the mathematically unique process of analytic continuation in the variable $1/T$, for the quantities 4.1 and 4.2, from the positive to the negative real axis.

(3) The σ^* curve is somewhat asymmetric, extending farther to the high-ψ side of its maximum than to the low-ψ side. This asymmetry may relate to the expectation that poorly packed, high-enthalpy inherent structures are likely to possess anomalously low density.

(4) The curvature of $\sigma^*(\psi)$ is negative over its range of definition. Given observation (E) in section II, $\psi_m^*(T)$ can be located by the unique point of tangency between σ^* and a straight line with slope $\beta = (k_B T)^{-1}$.

In connection with this last point, Figure 2 explicitly indicates the tangency points accessed at the OTP thermodynamic melting temperature $T_m = 329.35$ K, boiling temperature $T_b = 605.2$ K, and the glass transition temperature $T_g = 240$ K. Table 1 indicates the numerical values of $\psi - \psi^{(cr)}$ and σ^* at these distinguished points, as well as for infinite temperature, and for the two temperatures at which σ^* vanishes, the apparent Kauzmann temperature T_K and its negative-temperature image T_{AK} ("anti-Kauzmann" temperature).

V. Discussion

Entries in Table 1 indicate that as liquid OTP is supercooled from T_m to T_g, the mean depth of inhabited amorphous basins declines substantially. However, kinetic arrest at the glass transition prevents the material from finding the deepest amorphous minima, predicted by the analysis to lie about 3800 J mol^{-1} above the crystalline absolute minimum. Supercooling

TABLE 1: Numerical Values for Distinguished Points along the σ^* Curve of Figure 2

T, K	$\psi - \psi^{(cr)}$, J mol^{-1}	σ^*	exp(σ^*)
202.79 (T_K)	3797.5	0	1
240 (T_g)	8337.2	2.4762	11.896
329.35 (T_m)	17 191.0	6.2779	532.67
605.2 (T_b)	32 741.7	10.5805	39 360
∞	60 354.5	13.1397	508 744
-369.05 (T_{AK})	134 269.5	0	1

experimentally succeeds in moving the system only about 66% toward that "ideal glass state".[21]

The last column of Table 1, exp (σ^*), expresses the density of isobaric inherent structures as an equivalent degeneracy factor per molecule. That this single-molecule factor should rise to approximately 5×10^5 at the σ^* maximum might seem surprising at first sight. However it should be recalled that each OTP molecule has at least nine degrees of freedom that are relevant to the creation of mechanically stable packings, the inherent structures. Furthermore the packings that are typical for the neighborhood of the σ^* maximum ($T \rightarrow \infty$) will have low density, presumably permitting substantially more packing options than at high density.

The detailed behavior of the σ^* curve shown in Figure 2 near its low-ψ terminus may not be qualitatively correct. An argument has been advanced[15] suggesting that, as a result of possible localized rearrangements in the lowest-ψ amorphous structure, σ^* should have an infinite slope at this point. If such an alternative were true, the concept of an ideal glass transition at a precisely defined positive temperature T_K would not hold up to absolutely rigorous analysis. Nevertheless, the Kauzmann temperature remains a useful empirical concept (particularly for fragile glass formers such as OTP) that helps to summarize behavior in the deeply supercooled regime of the liquid state.

Given $\sigma^*(\psi)$ for inherent structures that are subject to a noncrystallinity restriction, it is trivial to reconstitute $\sigma(\psi)$ for the full and unrestricted set of inherent structures. All that is required is a "single tangent construction", roughly analogous to the Maxwell double tangent construction of equilibrium phase transition thermodynamics.[22] A straight line segment passing through the origin in Figure 2 ($\psi = \psi^{(cr)}$) will be tangent to σ^* at $\psi_m^*(T_m)$, the melting point location indicated. σ is given by this straight line segment, and σ^* for larger ψ.

A tentative conclusion can be advanced about the relative shape expected for $\sigma^*(\psi)$ in the case of a glass former such as SiO_2 that is at the opposite "strong" extreme.[1−3] In order that the liquid heat capacity be much closer to that of the crystal (one of the characteristics of the "strong" category), rolling of the tangent line of slope $\beta = (k_B T)^{-1}$ on the σ^* curve must entail relatively little ψ change. The only way this can arise is for the distribution represented by σ^* to be much narrower in ψ than it is for the fragile extreme.

Finally, it must be emphasized that knowledge of σ^* alone does not directly lead to predictions of transport and relaxational properties, such as shear viscosity and inelastic light scattering. These attributes depend on the way that inherent structures and their associated basins are arranged in the multidimensional configuration space and upon the height distribution of intervening barriers.[13,23] An additional physical assumption must be appended in order to penetrate the domain of time-dependent glass properties; the Adam−Gibbs theory of relaxation and flow provides a well-known example.[24]

References and Notes

(1) Angell, C. A. In *Relaxations in Complex Systems*; Ngai, K., Wright, G. B., Eds.; National Technical Information Service: U.S. Department of Commerce, Springfield, VA, 1985; p 1.
(2) Angell, C. A. *J. Non-Cryst. Solids* **1991**, *131*−*133*, 13.
(3) Angell, C. A. *Science* **1995**, *267*, 1924.
(4) Birkett Clews, C. J.; Lonsdale, K. *Proc. R. Soc. A* **1937**, *161*, 493.
(5) Aikawa, S.; Maruyama, Y.; Ohashi, Y.; Sasada, Y. *Acta Crystallogr. B* **1978**, *34*, 2901.
(6) Chang, S. S.; Bestul, A. B. *J. Chem. Phys.* **1972**, *56*, 503.
(7) Laughlin, W. L.; Uhlmann, D. R. *J. Phys. Chem.* **1972**, *76*, 2317.
(8) Plazek, D.; Bero, C. A.; Chay, I.-C. *J. Non-Cryst. Solids* **1994**, *172*−*174*, 181.
(9) Dixon, P. K.; Nagel, S. R. *Phys. Rev. Lett.* **1988**, *61*, 341.
(10) Fytas, G.; Wang, C. H.; Lilge, D.; Dorfmüller, Th. *J. Chem. Phys.* **1981**, *75*, 4247.
(11) Fujara, F.; Geil, B.; Sillescu, H.; Fleischer, G. *Z. Phys. B: Condens. Matter* **1992**, *88*, 195.
(12) Jäckle, J. *Rep. Prog. Phys.* **1986**, *49*, 171.
(13) Stillinger, F. H. *Science* **1995**, *267*, 1935.
(14) Kauzmann, W. *Chem. Rev.* **1948**, *43*, 219.
(15) Stillinger, F. H. *J. Chem. Phys.* **1988**, *88*, 7818.
(16) Stillinger, F. H.; Weber, T. A. *Phys. Rev. A* **1982**, *25*, 978.
(17) Stillinger, F. H.; Weber, T. A. *Science* **1984**, *225*, 983.
(18) Stillinger, F. H. *Phys. Rev. E*, to be published.
(19) Stillinger, F. H. *J. Chem. Phys.* **1988**, *88*, 380.
(20) Häner, P.; Schilling, R. *Europhys. Lett.* **1989**, *8*, 129.
(21) Angell, C. A.; MacFarlane, D. R.; Oguni, M. *Ann. N. Y. Acad. Sci.* **1986**, *484*, 241.
(22) Huang, K. *Statistical Mechanics*; Wiley: New York, 1963; pp 44−46.
(23) Stillinger, F. H. *Physica D* **1997**, *107*, 382.
(24) Adam, G.; Gibbs, J. H. *J. Chem. Phys.* **1965**, *43*, 139.